

# Superconducting gap in $\text{BaFe}_2(\text{As}_{1-x}\text{P}_x)_2$ from temperature dependent transient optical reflectivity

A. Pogrebna,<sup>1,2</sup> T. Mertelj,<sup>1,3,\*</sup> Z. R. Ye,<sup>4</sup> D. L. Feng,<sup>4</sup> and D. Mihailovic<sup>1,2,3</sup>

<sup>1</sup>Complex Matter Dept., Jozef Stefan Institute, Jamova 39, Ljubljana, SI-1000, Ljubljana, Slovenia

<sup>2</sup>Jožef Stefan International Postgraduate School, Jamova 39, SI-1000 Ljubljana, Slovenia

<sup>3</sup>CENN Nanocenter, Jamova 39, Ljubljana SI-1000, Slovenia

<sup>4</sup>State Key Laboratory of Surface Physics, Key Laboratory of Micro and Nano Photonic Structures (Ministry of Education), Department of Physics, and Advanced Materials Laboratory, Fudan University, Shanghai 200433, China

(Dated: 29th June 2021)

Temperature and fluence dependence of the 1.55-eV optical transient reflectivity in  $\text{BaFe}_2(\text{As}_{1-x}\text{P}_x)_2$  was measured and analysed in the low and high excitation density limit. The effective magnitude of the superconducting gap of  $\sim 5$  meV obtained from the low-fluence-data bottleneck model fit is consistent with the ARPES results for the  $\gamma$ -hole Fermi surface. The superconducting-state nonthermal optical destruction energy was determined from the fluence dependent data. The in-plane optical destruction energy scales well with  $T_c^2$  and is found to be similar in a number of different layered superconductors.

## I. INTRODUCTION

In iron pnictides the superconductivity appears from parent spin density wave (SDW) antiferromagnetic state as a result of doping or application of external pressure/strain. In  $\text{BaFe}_2(\text{As}_{1-x}\text{P}_x)_2$  the superconducting (SC) state is induced by means of the chemical strain induced by the isovalent substitution of arsenic by phosphorous. In optimally doped  $\text{BaFe}_2(\text{As}_{0.7}\text{P}_{0.3})_2$ , where the critical temperature reaches  $T_c = 30$  K, the SC gaps were thoroughly analysed by means of angle-resolved photoemission spectroscopy<sup>1</sup> (ARPES). Contrary to the optimally doped  $\text{Ba}(\text{Fe}_{1-x}\text{Co}_x)_2\text{As}_2$ , where there is little indication of nodes<sup>2,3</sup>, nodes in the SC gap were clearly observed<sup>1,4</sup> in  $\text{BaFe}_2(\text{As}_{0.7}\text{P}_{0.3})_2$ .

To study a possible effect of the nodes on the photoexcited quasiparticle relaxation and to supplement the ARPES<sup>1</sup> results on the SC gap sizes with a more bulk-sensitive technique we therefore conducted a systematic 1.55-eV optical transient reflectivity study in optimally doped  $\text{BaFe}_2(\text{As}_{0.7}\text{P}_{0.3})_2$ . It was found that similarly to the SC cuprates the nodes do not suppress the formation of the Rothwarf-Taylor<sup>5,6</sup> relaxation bottleneck. The behaviour is consistent with previous time-resolved optical spectroscopy data<sup>7,8</sup> in related electron doped  $\text{BaFe}_2\text{As}_2$  (Ba-122), together with the presence of the normal-state pseudogap. The effective SC gap obtained from the low-fluence linear-response data is consistent with the ARPES results.<sup>1</sup>

## II. EXPERIMENTAL DETAILS

Single crystals of  $\text{BaFe}_2(\text{As}_{0.7}\text{P}_{0.3})_2$  were grown from self flux at Fudan University.<sup>1</sup> A sample from the same batch as the one used for our experiment showed the onset of superconductivity at  $T_C = 30$  K as determined by the SQUID susceptibility and electric transport measurements. For optical measurements the crystal was glued

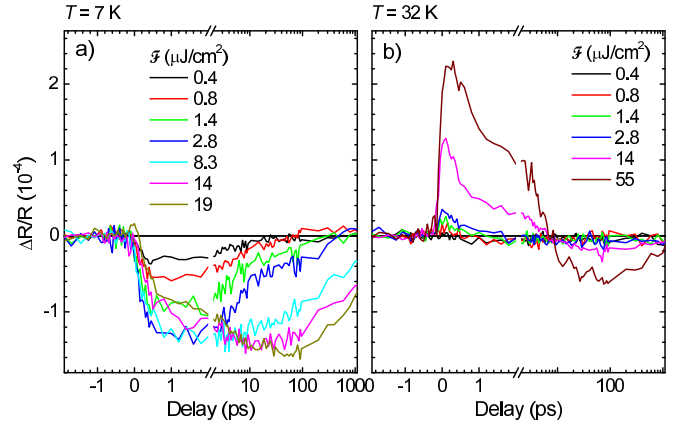


Figure 1. Photoinduced reflectivity transients  $\Delta R/R$  in  $\text{BaFe}_2(\text{As}_{0.7}\text{P}_{0.3})_2$  measured in the superconducting state (a) and normal state (b) as a function of the pump fluence.

onto a copper sample holder and cleaved by a razor blade before mounting into an optical liquid-He flow cryostat.

Measurements of the transient photoinduced reflectivity,  $\Delta R/R$ , were performed using the standard pump-probe technique, with 50 fs optical pulses from a 250-kHz Ti:Al<sub>2</sub>O<sub>3</sub> regenerative amplifier seeded with an Ti:Al<sub>2</sub>O<sub>3</sub> oscillator. We used the pump and probe photons with the laser fundamental ( $\hbar\omega_P = 1.55$  eV) photon energy. An analyser oriented perpendicularly to the pump beam polarization was used for rejection of the pump scattered light. The pump and probe beams were nearly perpendicular to the cleaved sample surface (001) with polarizations perpendicular to each other. The beam diameters were calibrated by measuring the transmission through a set of different size pinholes mounted at the sample position.

### III. RESULTS

In Fig. 1 we show the pump fluence ( $\mathcal{F}$ ) dependence of the transient reflectivity in the SC state ( $T = 7$  K) compared with the normal state transients measured just above  $T_c$  ( $T = 32$  K). The signals show no significant pump and probe polarization dependence. In the SC state the amplitude of the signal depends linearly on  $\mathcal{F}$  at low fluences and saturates with increasing fluence above  $\sim 3\mu\text{J}/\text{cm}^2$ . The normal-state response shown in Fig. 1 (b) appears much weaker at low fluencies with a different sign and a faster relaxation time in comparison to the SC response. At high fluencies, above  $\sim 10\mu\text{J}/\text{cm}^2$ , the magnitude of the normal state response becomes comparable to the SC-response magnitude due to saturation of the SC-response.

In Fig. 2 we show the temperature dependence of the transient reflectivity at two selected fluences. The lower was chosen to be in the  $\mathcal{F}$ -linear SC-response region in most of the  $T$  range while the higher corresponds to the strongly saturated SC-response fluence. In both cases the data in the normal state collapse on a single curve in a wide  $T$  range up to twice the  $T_c$  suggesting a  $T$ -independent background response present also in the SC state. We subtract this normal-state background response to obtain the SC-state response, as shown in Fig. 2 (c) and (d). At the low fluence the subtraction does not significantly change the shape of the response while at the high fluence it leads to the complete removal of the sub-picosecond timescale dynamics, which is associated with the normal state response, justifying the subtraction procedure.

The SC-response shows a  $\sim 0.5$  ps risetime followed by  $\sim 5$  ps decay time at the low excitation. At the high excitation the risetime is faster on  $\sim 0.2$  ps timescale while the relaxation slows down to nanosecond timescale. In both cases the relaxation slows down when approaching  $T_c$  from below.

### IV. DISCUSSION

#### A. Excitation density dependence

The saturation behaviour of the transient-reflectivity amplitude with increasing excitation density was observed in a number of gapped systems such as superconductors<sup>8-14</sup> and charge-density wave compounds<sup>15,16</sup>. The saturation of the transient reflectivity amplitude was associated with a nonthermal destruction of the condensate and complete closure of the gap. Due to an inhomogeneous excitation resulting from a finite light penetration depth and finite beam diameters the exact shape of the amplitude versus  $\mathcal{F}$  curve depends on geometrical parameters. In order to obtain the bulk SC state destruction energy density,  $U_d$ , we therefore use the inhomogeneous SC-state destruction model<sup>9</sup> to fit the fluence dependence of

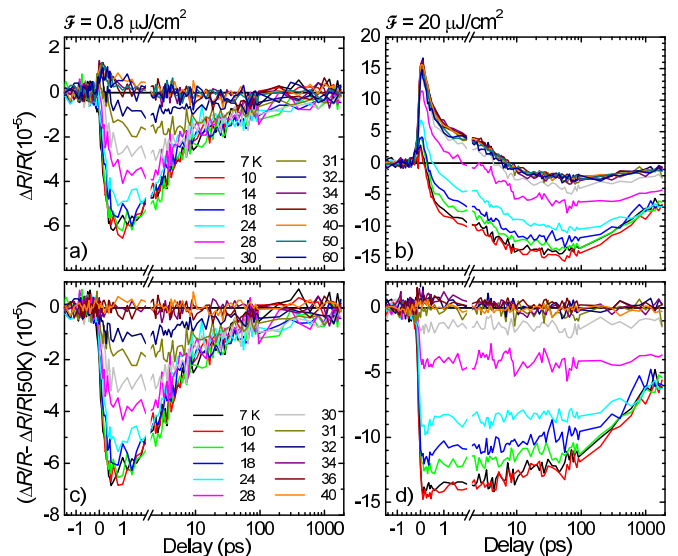


Figure 2. Temperature dependence of the transient reflectivity  $\Delta R/R$  at low (a) and high (b) fluence. Note that the data above the critical temperature collapse on a single curve in a wide temperature range at both fluencies. The superconducting state response obtained by subtracting the average of the transients from the 34 K - 50 K interval at low (c) and high (d) fluence.

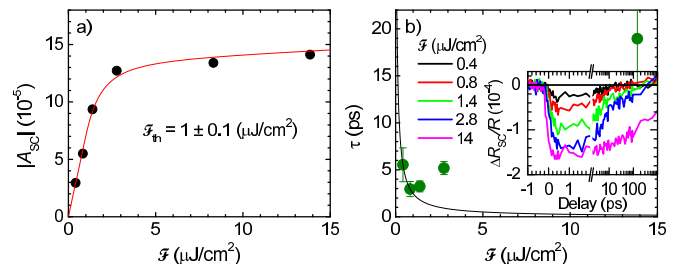


Figure 3. (a) The fluence dependence of the transient amplitude at  $T = 7$  K. The thin line in is the saturation model<sup>9</sup> fit discussed in text. (b) The dominant relaxation time in the superconducting state ( $T = 7$  K). The thin line in is the Rothwarf-Tyaltor fit<sup>6</sup>. The inset to (b) shows the 7-K transients with the 32-K normal state response subtracted.

the transient reflectivity amplitude and determine the external SC state destruction threshold fluence,  $\mathcal{F}_{th} = 1 \pm 0.1 \mu\text{J}/\text{cm}^2$  [see Fig. 3 (a)]. The bulk SC state destruction energy density required to completely destroy the superconducting state is then obtained as  $U_d/k_B = \mathcal{F}_{th}(1 - R)/\lambda_p = 0.68$  K/Fe, where  $\lambda_p = 34$  nm is the light penetration depth and  $R = 0.37$  the reflectivity at 1.55-eV photon energy taken from data<sup>17</sup> on related Co doped Ba-122. As previously noted<sup>8</sup> this value is much smaller than the energy needed to heat the sample thermally above  $T_c$  indicating that the SC destruction is highly nonthermal.

In Fig. 4 we compare the SC-condensate optical de-

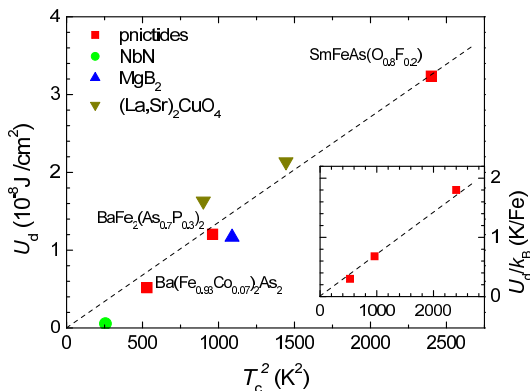


Figure 4. The in-plane<sup>18</sup> SC-state optical destruction energy density as function of  $T_c^2$  for some iron based pnictides compared to NbN<sup>20</sup>, MgB<sub>2</sub><sup>21</sup> and (La,Sr)<sub>2</sub>CuO<sub>4</sub><sup>9</sup>. The inset shows  $U_d$  in pnictides normalized to the Fe content.

struction energy in iron pnictides with some other superconductors. As discussed previously<sup>12</sup>  $U_d$  is roughly proportional to  $T_c^2$ . The actual value for each compound depends on the thermodynamic condensation energy and the amount of the energy lost by transfer to the non-pair-breaking subgap phonons<sup>12</sup>. It is therefore somewhat surprising that the in-plane<sup>18</sup> destruction-energy densities for very different layered compounds lie rather close to the same line with the exception of the three dimensional NbN.

Within the iron-pnictide class the accuracy of the scaling with  $T_c^2$  is enhanced if one considers the optical destruction energy normalized to the Fe content (see inset to Fig. 4). This suggests that the differences of the detailed gap structure<sup>19</sup> between different members contribute only a small correction to the free-energy gain in the SC state.

## B. Temperature dependence and the SC gap

Far above the saturation  $\mathcal{F}$  the transient reflectivity on short timescales can be understood as the difference between the SC and normal state reflectivities and can be described in terms of the high frequency limit of the Mattis-Bardeen formula<sup>22</sup>:

$$\Delta R_{\text{SC}} \propto \left( \frac{\Delta(T)}{\hbar\omega} \right)^2 \ln \left( \frac{3.3\hbar\omega}{\Delta(T)} \right) \quad (1)$$

where  $\hbar\omega$  is the photon energy and  $\Delta(T)$  is a temperature dependent gap. Using the BCS temperature dependent gap<sup>23</sup> the formula fits well the temperature dependence of the transient reflectivity amplitude measured in the strong excitation regime as shown in Fig. 5 (b).

In the weak perturbation limit the transient optical response of superconductors was shown to be governed by the phonon bottleneck effects.<sup>5–7,24</sup> The dynamics is usually discussed in the framework of simple effective

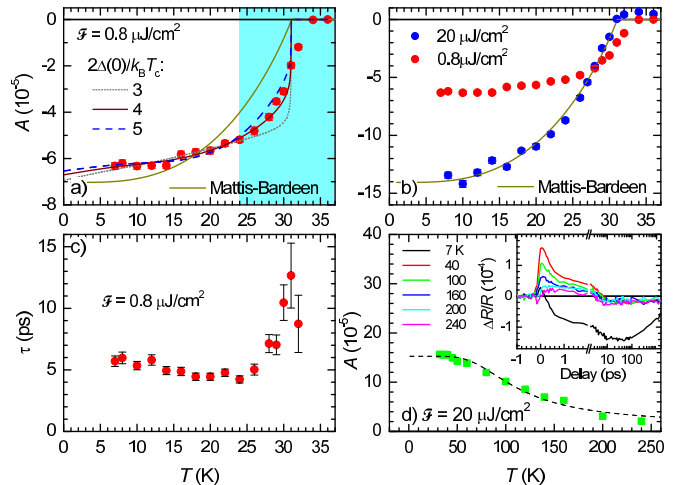


Figure 5. The temperature dependence of the SC response amplitude for low (a) and high (b) excitation density. The lines are fits discussed in text, where the shaded region in (a) was excluded from the bottleneck model fits. (c) The low-excitation SC-response relaxation time as a function of temperature. (d) Temperature dependence of the normal-state transient reflectivity amplitude. The dashed line is a bottleneck fit with  $T$ -independent gap. Transients at a few characteristic temperatures are shown in the inset.

two-electronic-level models such as the Rothwarf-Taylor model<sup>5</sup> and the related Kabanov bottleneck model<sup>24</sup>. Both enable determination of the characteristic SC gap energy from the  $T$ -dependent transient response amplitude.<sup>6,24</sup>

The weak excitation limit is difficult to achieve in the case of iron pnictides due to rather small transient reflectivity magnitudes and low optical destruction thresholds. In the present case the lowest fluence of  $0.8 \mu\text{J}/\text{cm}^2$  used for  $T$ -scans appears to be near the limit of the  $\mathcal{F}$ -linear response region. The  $\mathcal{F}$ -dependent dominant<sup>25</sup> relaxation time shown in Fig. 3 (b) shows the expected Rothwarf-Taylor behaviour,<sup>6</sup>  $\tau = \tau_0(\mathcal{F} + \mathcal{F}_T)^{-1}$ , below  $\mathcal{F} \sim 0.8 \mu\text{J}/\text{cm}^2$  only, with  $\mathcal{F}_T = 0.05 \mu\text{J}/\text{cm}^2$  at 7K, where  $\mathcal{F}_T$  corresponds to the fluence at which the density of the photoexcited quasiparticles is comparable to the thermally excited quasiparticle density.

On the other hand, the amplitude of the response appears almost linear up to  $\mathcal{F} \sim 1.4 \mu\text{J}/\text{cm}^2$  at the lowest  $T$  while the  $\mathcal{F}=0.8\text{-}\mu\text{J}/\text{cm}^2$  amplitude reaches the saturation value only above  $T \sim 28\text{K}$  [see Fig. 5 (b)]. We therefore assume that for  $T \lesssim 25\text{K}$  the response is  $\mathcal{F}$ -linear and the  $T$ -dependent amplitude,  $A(T)$ , is proportional to the low- $\mathcal{F}$  limit and follows the bottleneck model from Kabanov *et al.*<sup>24</sup>,

$$A(T) \propto n_{pe} \propto \left[ \left( \frac{2\Delta(T)}{k_B T_c} + \frac{T}{T_c} \right) \left( 1 + g_{ph} \sqrt{\frac{k_B T}{\Delta(T)}} \exp\left(-\frac{\Delta(T)}{k_B T}\right) \right) \right]^{-1}, \quad (2)$$

where  $g_{ph}$  represents the relative effective number of the involved phonon degrees of freedom. Fitting  $A(T)$  in Fig. 5 (a) using (2) with the BCS temperature dependent gap,  $\Delta(T)$ , we obtain  $2\Delta(0)/k_B T_c = 4 \pm 1$ , with  $\Delta(0) \sim 5$  meV. This value is consistent with the gap on the  $\gamma$  hole Fermi surface and smaller than the gap on the electron Fermi surfaces as obtained by ARPES<sup>1</sup> in the samples from the same batch. The relaxation dynamics detected by means of 1.55-eV probe photons in  $\text{BaFe}_2(\text{As}_{1-x}\text{P}_x)_2$  can therefore be attributed to the hole Fermi surfaces as suggested<sup>7</sup> for K and Co doped Ba-122.

Despite the presence of several bands with different gaps in the case of iron based pnictides and the presence of the gap node<sup>1</sup> on the  $\alpha$  hole Fermi surface in  $\text{BaFe}_2(\text{As}_{1-x}\text{P}_x)_2$  the amplitude of the weak-excitation response in the SC state seems to be reasonably well described by the bottleneck model similarly to the cuprate superconductors.<sup>6</sup>

The weak-excitation divergence of the relaxation time of the SC signal at  $T_c$  [see Fig. 5 (c)] can also be well described by the bottleneck model.<sup>24</sup> In the proximity to the transition temperature the SC gap becomes smaller, which means that the probability to find a boson with the energy higher than the gap size becomes higher and this slows down the relaxation of photoexcited quasiparticles. The low-T divergence, predicted by the Rothwarf-Taylor model,<sup>6</sup> is, on the other hand, cut off by the rather high excitation density  $\mathcal{F} \gg \mathcal{F}_T$ .

At low excitation fluence we observe a measurable response up to 2 K above  $T_c = 30$  K, which vanishes at the highest fluence. We attribute this response to SC fluctuations<sup>26</sup> although we can not rule out a +1 K error in the determination of the sample  $T$ <sup>23</sup>. This error does not significantly affect the gap determination from the fit (2) above.

The normal state sub-ps transient response, which shows a vanishing amplitude with increasing temperature disappearing around  $T = 200$  K, is very similar to the behaviour in Co-doped Ba-122<sup>8</sup>, where it was associated with the presence of the pseudogap due to the nematic fluctuations. It is plausible to assume that the origin is the same in the present case. The temperature range of

vanishing pseudogap is about 50 K above the pseudogap formation temperature based on ARPES results<sup>27</sup>. Contrary to Co-doped Ba-122 it does not show any 4-fold axis symmetry breaking. Since a global external symmetry breaking (strain) field is necessary to orient the fluctuations across the whole experimental volume along one direction this observation indicates the absence of a global field, but it does not rule out local fields with varying orientation enhancing the nematic fluctuations.

Using a bottleneck fit with a  $T$ -independent gap as in Ref. [8] we obtain the characteristic pseudogap magnitude,  $2\Delta_{PG} = 690 \pm 70$  K, which is within the errorbars identical to the magnitude ( $2\Delta_{PG} = 660 \pm 100$  K) in the optimally Co doped Ba-122.<sup>8</sup>

## V. CONCLUSIONS

Conducting a systematic wide-fluence-range optical time-resolved optical pump-probe study in optimally iso-valently doped  $\text{BaFe}_2(\text{As}_{0.7}\text{P}_{0.3})_2$  we find a similar behaviour to previously studied<sup>7,8</sup>  $\text{Ba}(\text{Fe},\text{Co})_2\text{As}_2$ .

The superconducting gap magnitude of  $2\Delta(0)/k_B T_c = 4 \pm 1$  is consistent with the gap on the  $\gamma$  hole Fermi surface. The relaxation dynamics detected by means of 1.55-eV probe photons in Ba-122 can therefore be attributed to the hole Fermi surfaces as suggested previously by Torchinsky *et al.* [7].

The normal state response indicates the presence of a pseudogap related to the nematic fluctuations up to  $T \sim 200$  K as generally observed in the electron doped iron based pnictide superconductors.

The in-plane<sup>18</sup> nonthermal optical-destruction volume energy densities are found to scale linearly with  $T_c^2$  and lie close to the same line for a range of different layered superconductors.

## ACKNOWLEDGMENTS

Work at Jozef Stefan Institute was supported by ARRS (Grant No. P1-0040).

\* tomaz.mertelj@ijs.si

<sup>1</sup> Y. Zhang, Z. Ye, Q. Ge, F. Chen, J. Jiang, M. Xu, B. Xie, and D. Feng, *Nature Physics* **8**, 371 (2012).

<sup>2</sup> K. Terashima, Y. Sekiba, J. H. Bowen, K. Nakayama, T. Kawahara, T. Sato, P. Richard, Y.-M. Xu, L. J. Li, G. H. Cao, Z.-A. Xu, H. Ding, and T. Takahashi, *Proceedings of the National Academy of Sciences* **106**, 7330 (2009)

<sup>3</sup> J.-P. Reid, M. A. Tanatar, X. G. Luo, H. Shakeripour, N. Doiron-Leyraud, N. Ni, S. L. Bud'ko, P. C. Canfield, R. Prozorov, and L. Taillefer, *Phys. Rev. B* **82**, 064501 (2010).

<sup>4</sup> J. S. Kim, P. J. Hirschfeld, G. R. Stewart, S. Kasahara, T. Shibauchi, T. Terashima, and Y. Matsuda, *Phys. Rev. B* **81**, 214507 (2010).

- <sup>5</sup> A. Rothwarf and B. N. Taylor, Phys. Rev. Lett. **19**, 27 (1967).
- <sup>6</sup> V. V. Kabanov, J. Demsar, and D. Mihailovic, Phys. Rev. Lett. **95**, 147002 (2005).
- <sup>7</sup> D. H. Torchinsky, J. W. McIver, D. Hsieh, G. F. Chen, J. L. Luo, N. L. Wang, and N. Gedik, Phys. Rev. B **84**, 104518 (2011).
- <sup>8</sup> L. Stojchevska, T. Mertelj, J. Chu, I. Fisher, and D. Mihailovic, Physical Review B **86**, 024519 (2012).
- <sup>9</sup> P. Kugar, V. Kabanov, J. Demsar, T. Mertelj, S. Sugai, and D. Mihailovic, Physical Review Letters **101**, 227001 (2008).
- <sup>10</sup> C. Giannetti, G. Coslovich, F. Cilento, G. Ferrini, H. Eisaki, N. Kaneko, M. Greven, and F. Parmigiani, Phys. Rev. B **79**, 224502 (2009).
- <sup>11</sup> T. Mertelj, P. Kugar, V. V. Kabanov, L. Stojchevska, N. D. Zhigadlo, S. Katrych, Z. Bukowski, J. Karpinski, S. Weyeneth, and D. Mihailovic, Phys. Rev. B **81**, 224504 (2010).
- <sup>12</sup> L. Stojchevska, P. Kugar, T. Mertelj, V. V. Kabanov, Y. Toda, X. Yao, and D. Mihailovic, Phys. Rev. B **84**, 180507 (2011).
- <sup>13</sup> G. Coslovich, C. Giannetti, F. Cilento, S. Dal Conte, G. Ferrini, P. Galinetto, M. Greven, H. Eisaki, M. Raichle, R. Liang, A. Damascelli, and F. Parmigiani, Phys. Rev. B **83**, 064519 (2011).
- <sup>14</sup> M. Beyer, D. Städter, M. Beck, H. Schäfer, V. V. Kabanov, G. Logvenov, I. Bozovic, G. Koren, and J. Demsar, Phys. Rev. B **83**, 214515 (2011).
- <sup>15</sup> A. Tomeljak, H. Schäfer, D. Städter, M. Beyer, K. Biljakovic, and J. Demsar, Phys. Rev. Lett. **102**, 066404 (2009).
- <sup>16</sup> R. V. Yusupov, T. Mertelj, P. Kugar, V. Kabanov, S. Brazovskii, J.-H. Chu, I. R. Fisher, and D. Mihailovic, Nature Physics **6**, 681 (2010).
- <sup>17</sup> N. Barišić, D. Wu, M. Dressel, L. J. Li, G. H. Cao, and Z. A. Xu, Phys. Rev. B **82**, 054518 (2010).
- <sup>18</sup> We normalize the energy density to a single FeAs, CuO<sub>2</sub>, Mg or Nd plane by multiplying the volume density by the interplane distances.
- <sup>19</sup> For example the presence of nodes in BaFe<sub>2</sub>(As,P)<sub>2</sub>.
- <sup>20</sup> M. Beck, M. Klammer, S. Lang, P. Leiderer, V. V. Kabanov, G. N. Gol'tsman, and J. Demsar, Phys. Rev. Lett. **107**, 177007 (2011).
- <sup>21</sup> J. Demsar, R. D. Averitt, A. J. Taylor, W.-N. Kang, H. J. Kim, E.-M. Choi, and S.-I. Lee, International Journal of Modern Physics B **17**, 3675 (2003).
- <sup>22</sup> D. C. Mattis and J. Bardeen, Phys. Rev. **111**, 412 (1958).
- <sup>23</sup> From the fit  $T_c = 31 \pm 0.2$  K was obtained which is 1 K higher than the maximum bulk  $T_c$  in this system. The difference can not be attributed to the thermal gradient due to the laser excitation and the room radiation thermal load since it should decrease the apparent  $T_c$ , but to an error in the cryostat  $T$  calibration, which was checked a posteriori by means of a calibrated diode temperature sensor mounted at the sample position to be  $\pm 1$  K.
- <sup>24</sup> V. V. Kabanov, J. Demsar, B. Podobnik, and D. Mihailovic, Phys. Rev. B **59**, 1497 (1999).
- <sup>25</sup> The relaxation at higher  $\mathcal{F}$  is clearly non exponential where the faster part can be associated with the Rothwarf-Taylor bottleneck, while the slower one corresponds to the cooling after all degrees of freedom have been thermalized.<sup>11</sup> At excitation densities above a few  $\mu\text{J}/\text{cm}^2$  the amount of absorbed optical energy is large enough to heat the phonon bath above  $T_c$  and the SC state recovery is governed by the energy escape from the probed volume.
- <sup>26</sup> I. Madan, T. Kurosawa, Y. Toda, M. Oda, T. Mertelj, P. Kugar, and D. Mihailovic, Sci. Rep. **4**, (2014).
- <sup>27</sup> T. Shimojima, T. Sonobe, W. Malaeb, K. Shinada, A. Chainani, S. Shin, T. Yoshida, S. Ideta, A. Fujimori, H. Kumigashira, K. Ono, Y. Nakashima, H. Anzai, M. Arita, A. Ino, H. Namatame, M. Taniguchi, M. Nakajima, S. Uchida, Y. Tomioka, T. Ito, K. Kihou, C. H. Lee, A. Iyo, H. Eisaki, K. Ohgushi, S. Kasahara, T. Terashima, H. Ikeda, T. Shibauchi, Y. Matsuda, and K. Ishizaka, Phys. Rev. B **89**, 045101 (2014).